Nonequilibrium polariton condensate in a magnetic field

C. Sturm,[1,*] D. Solnyshkov,[2] O. Krebs,[1] A. Lemaître,[1] I. Sagnes,[1] E. Galopin,[1] A. Amo,[1] G. Malpuech,[2] and J. Bloch[1]
[1]*Laboratoire de Photonique et Nanostructures, LPN/CNRS, Route de Nozay, 91460 Marcoussis, France*
[2]*Institut Pascal, Photon-N2, Université Clermont Auvergne and Université Blaise Pascal, CNRS, 63177 Aubière Cedex, France*
(Received 17 September 2014; revised manuscript received 16 March 2015; published 20 April 2015)

We investigate exciton-polariton condensation in a magnetic field in a single high-quality semiconductor micropillar cavity. We observe successive polariton condensation of each spin component for two distinct threshold powers. Pronounced and nonmonotonous variations of both the Zeeman splitting and the circular polarization of the emission are measured across these two condensation thresholds. This unexpected behavior deeply deviates from the so-called spin-Meissner effect predicted for a fully thermalized system. Our measurements can be understood in a kinetic approach taking into account spin-anisotropic interactions within the entire system: the polariton condensate and the cloud of uncondensed excitons.

DOI: 10.1103/PhysRevB.91.155130 PACS number(s): 71.36.+c, 71.35.Ji, 71.70.Ej, 78.55.Cr

I. INTRODUCTION

Manipulation of the laser emission using magnetic fields has remained elusive due to the weak magnetic response of photonic devices, particularly in the visible range. In the case of semiconductor vertical cavity surface emitting lasers (VCSELs), intrinsic birefringence due to anisotropies along the main crystal axes greatly reduces the influence of Zeeman or Faraday effects on the polarization of the lasing modes [1]. More generally, a substantial magnetic response could be of high interest for many photonic applications, such as the realization of photonic topological insulators [2,3], which so far are limited to the microwave range. An interesting strategy to enhance the response of a laser, and more generally of photonic devices to a magnetic field is to couple photons to matter excitations, sensitive to magnetic fields. One of the most suitable systems to achieve this are exciton-polaritons in semiconductor microcavities. Polariton condensates preserve the intensity and coherence properties of optically pumped VCSELs while, in addition, present both significant magnetic response [4–7] and interactions not only among themselves but also with the excitonic reservoir that feeds them [8]. Since the strong light-matter coupling spectrally pushes polariton states away from dark $J = 2$ excitons, polariton interactions, governed by exchange interactions, are strongly spin anisotropic [9]. More precisely, the polariton-polariton interaction constant α_1 for polaritons with parallel spins is different and in general much stronger than α_2, the interaction constant for polaritons with opposite spins. The strength of these interactions can vary strongly when polaritons undergo Feshbach resonance with the biexciton [10]. All these properties provide a rich playground to manipulate polariton condensates and their polarization with a magnetic field.

Up to now, the spin degree of freedom in polariton condensates under nonresonant excitation has been mainly considered under the assumption of thermodynamic equilibrium between the spin species and negligible condensate depletion. In the absence of an external magnetic field, one of the consequences of spin anisotropic interactions is that a polariton condensate must be linearly polarized [11–13] with an energy difference between a circularly and a linearly polarized condensate given by $(\alpha_1 - \alpha_2)n_c/2$ where n_c is the condensate density. In a magnetic field, it has been predicted that the spin-anisotropic interactions should screen the polariton Zeeman splitting (ZS) arising from the excitonic component [14]. The suppression of the Zeeman splitting appears as an expulsion of the magnetic field, and therefore is frequently referred to as spin-Meissner effect in analogy with the physics of superconductors. As a result, the chemical potential does not depend on the field up to a critical value B_c, and the polarization of the emission evolves from linear at zero field to circular at B_c. For fields larger than B_c, a Zeeman-like splitting should reappear.

Despite the intensive search for the observation of such phenomenon, no conclusive experimental evidence has been provided. Polariton condensation in an applied magnetic field oriented along the growth axis has been reported either under resonant excitation [15], where the thermal equilibrium condition cannot be fulfilled directly, or at very negative detuning [16,17], where the characteristics of the system are close to those of VCSELs in the weak coupling regime [1]. Additionally, the observed ZSs are smaller than the linewidth and thus difficult to measure precisely. In all cases, lasing is observed not in the ground state but in excited spin states, indicating that the system is out of thermal equilibrium. In such a regime, the steady state is defined by the kinetic equilibrium between pump, phonon-induced relaxation, polariton-polariton scattering, and losses [18–22], which contradicts one of the basic requirements of the spin-Meissner effect: quasithermodynamic equilibrium [14].

In this paper, we report on polarization-resolved emission measurements performed at high magnetic field on a polariton condensate in a GaAs-based semiconductor microcavity. We observe a nonmonotonous dependence of the ZS and polarization as a function of the excitation density. We show that the effects of the magnetic field are dominated by mechanisms neglected in previous works [16,17], namely the condensate depletion and spin-dependent interactions of polaritons with the excitonic reservoir. These effects combined with the slow spin relaxation previously considered [17,23,24] pushes the two spin subsystems out of their mutual equilibrium. While our results evidence the difficulties posed by the observation of the spin-Meissner effect in this type of microcavities, they provide

*Present address: Institut für Experimentelle Physik II, Universität Leipzig, Linnéstr. 5, 04103 Leipzig, Germany.

an interesting scheme to manipulate the spin (polarization) of the coherent light emitted from a microcavity.

II. EXPERIMENTAL DETAILS

Our sample, described in detail in Ref. [25], is a $\lambda/2$ cavity with a quality factor exceeding 16000 containing 12 GaAs quantum wells (Rabi splitting $\Omega = 15$meV). The micropillar under investigation has a square shape with 3.2 μm sides [Fig. 1(a)]. It was designed using electron beam lithography and dry etching. The exciton-photon detuning used in the experiments was about -2.4 meV, which corresponds to an excitonic content x larger than 40% [26]. The sample is immersed in superfluid helium ($T = 1.8$ K), together with a motorized lens used for excitation and collection, within a magneto-optics cryostat. A magnetic field up to $B = 9$ T was applied in the Faraday configuration. The nonresonant excitation was provided by a monomode cw Ti:Sapphire laser tuned typically 100 meV above the polariton resonances, linearly polarized and focused onto the sample with a spot size around 2 μm. The emission was collected in a confocal configuration and sent to a CCD camera coupled to a double monochromator. The polariton spin degree of freedom was probed by measuring the circular polarization of the emission [9].

III. EXPERIMENTAL RESULTS

Figure 1(a) shows the polarization-resolved emission spectra measured at $B = 9$T for several excitation powers. For the lowest power, several narrow emission lines are observed,

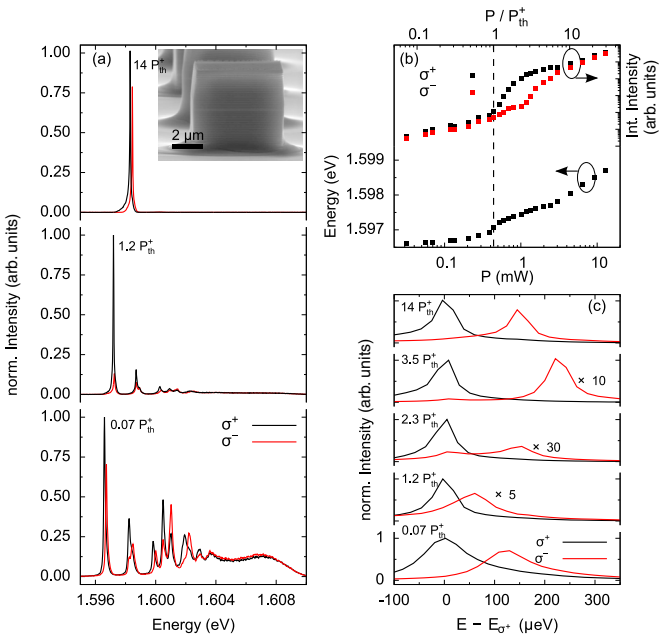

FIG. 1. (Color online) (a) Emission spectra measured under circular polarization for three different excitation powers ($P_{th}^+ = 0.44$ mW). (Inset) Scanning electron microscopy image of a micropillar cavity with an edge length of 6 μm; (b) (top) Integrated intensity for both circular polarizations and (bottom) energy of the σ^+ polariton mode as a function of excitation power. (c) Emission spectra measured under circular polarization for several excitation powers shown in smaller energy scale. For each power, the zero energy corresponds to the σ^+ polariton energy. $B = 9$ T

each of them corresponding to a well-defined discrete polariton state, confined within the micropillar. As the excitation power is increased, a strong nonlinear rise of the emission is observed, first σ^+ polarized (above $P_{th}^+ = 0.44$ mW), and then for the σ^- component (above $P_{th}^- = 1.06$ mW $= 2.4 P_{th}^+$). For each circular polarization, the emission is dominated by the lowest-energy polariton mode. Importantly, as seen in Fig. 1(b) the emission energy undergoes a continuous blueshift when increasing the excitation power, without discontinuity at threshold: this is a key feature allowing to conclude on polariton condensation.

The first hints of the peculiar behavior of polariton lasing under magnetic field can be seen in Fig. 1(c), which presents the emission spectra within a narrower energy range both for σ^+ and σ^- polarizations. For each excitation power, the ZS is clearly resolved, as it is significantly larger than the polariton linewidth. Strong variations of the ZS are observed when crossing the two condensation thresholds, at $P = P_{th}^+$ and $P = P_{th}^-$.

The variation of the ZS with excitation density is correlated with the emitted intensity in each component and with the degree of circular polarization, as summarized in Fig. 2 for three values of the magnetic field. Let us first describe in detail the measurements performed at 9 T. Below P_{th}^+, the measured circular polarization degree is almost constant, of the order of 0.2 [see Fig. 2(i)]. Approaching P_{th}^+, the ZS decreases from 130 μeV down to a minimum of 45 μeV [see Fig. 2(f)] which is reached slightly above P_{th}^+. Further increasing the excitation density above P_{th}^+, the emission becomes strongly circularly polarized (up to 96%). Surprisingly, and in contradiction with the spin-Meissner effect prediction, this is accompanied by a strong increase of the ZS. There is no clear correlation between the circular polarization degree of the emission and the ZS. The maximum ZS is reached for P close to P_{th}^- and amounts to 230 μeV, a value significantly larger than the initial one. For larger excitation power, a continuous decay of the ZS is observed down to its initial value, whereas the circular polarization degree goes to zero. As shown in Fig. 2, the difference $P_{th}^- - P_{th}^+$ between the two condensation threshold powers increases with magnetic field, and the behavior of both polarization ratio and ZS described above, develops progressively, as the magnetic field increases. We note, that for a positive detuning of about 2 meV a similar behavior as described above for the ZS and degree of circular polarization was observed.

IV. MODEL AND DISCUSSION

In the following, we propose a model to describe these unexpected variations of the ZS across the condensation threshold. We use a kinetic approach, similar to the one presented in Ref. [27] but including the different spin states and their mutual interaction. We consider the coupled kinetics of four effective states, namely the two spin components of the excitonic reservoir and the lowest-energy polariton state. Both exciton reservoirs are assumed to be at the internal thermal equilibrium and their energies are given by (see Appendix A)

$$E_r^{\pm} = E_{r_0} \mp 0.5\,\mu_B g B + \alpha_1(n_r^+ + n_r^- + x n_p^{\pm}) + 2\alpha_2 x n_p^{\mp} \quad (1)$$

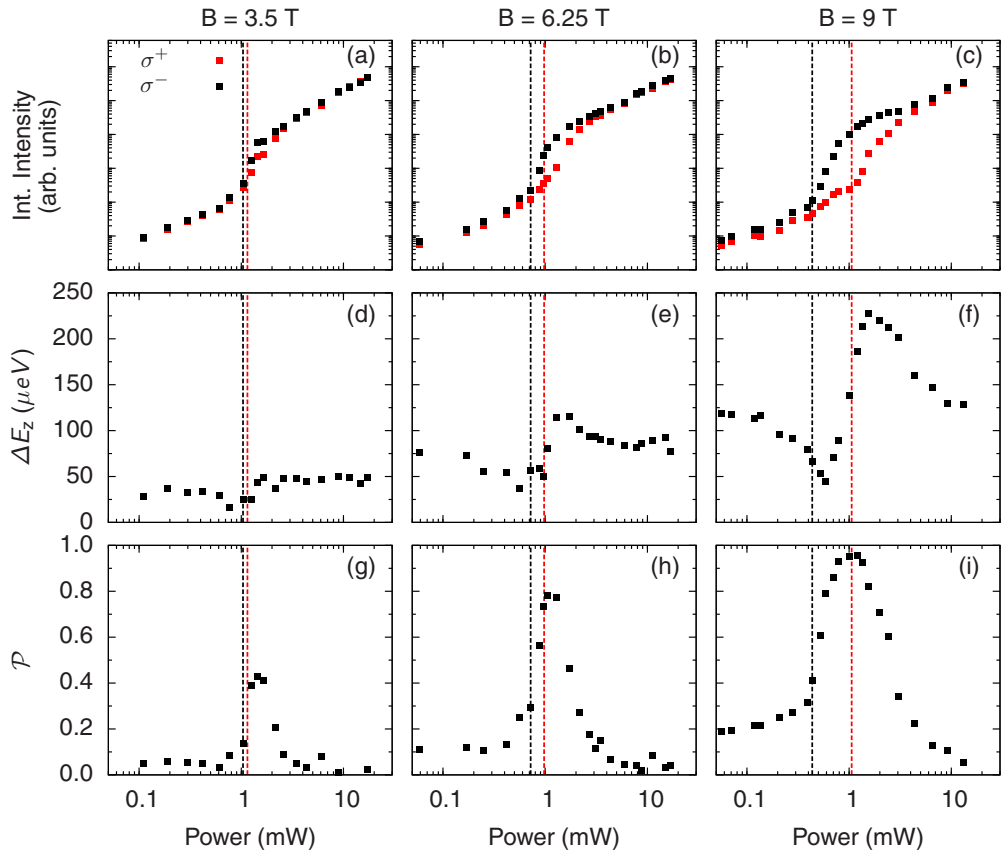

FIG. 2. (Color online) (a)–(c) Integrated intensity for both circular polarizations, (d)–(f) Zeeman splitting and (g)–(i) circulation polarization ratio measured as a function of power for three values of the magnetic field. The vertical dashed lines indicate condensation threshold for both circular polarizations.

where E_{r_0} is the reservoir energy at $B = 0$, $\mu_B g B$ the exciton ZS, $n_r^{\pm}$ the reservoir occupancy for each spin component, $n_p^{\pm}$ the occupation of the polariton state and x their exciton fraction, which for simplicity is assumed to be spin independent. The two excitonic reservoirs are coupled to each other through a spin conversion rate (spin relaxation due, for example, to the Dyakonov-Perel mechanism) [28,29]. They are also coupled to the polariton state with the same spin with an energy given by

$$E^{\pm} = E_{r_0} - \Delta \mp 0.5\, x\mu_B g B + \alpha_1 x(n_r^{\pm} + x n_p^{\pm}) + x\alpha_2(n_r^{\mp} + x n_p^{\mp}), \tag{2}$$

where $E_{r_0} - \Delta$ is the lowest polariton energy at $B = 0$ [26]. In the present experiment $\Delta \simeq 10$ meV, which means that polariton states are about 10 meV away from excitonic states (such as biexcitons for instance). Therefore we do not expect strong variations of α_1 and α_2 versus experimental parameters (as recently reported [10,30]). In our simulations, α_1 and α_2 are taken as constant with $|\alpha_2|$ at least an order of magnitude smaller than $|\alpha_1|$.

The time evolution of the occupation of the states is described by the following set of semiclassical Boltzmann equations:

$$\frac{dn_p^{\pm}}{dt} = W_{\mathrm{XX}}(n_r^{\pm})^2(n_p^{\pm}+1) - W_{\mathrm{XX}} D n_r^{\pm} n_p^{\pm} e^{\frac{E^{\pm}-E_r^{\pm}}{k_B T}} - n_r^{\pm}/\tau_{\mathrm{pol}} \tag{3}$$

$$\frac{dn_r^{\pm}}{dt} = W_{\mathrm{XX}} D n_r^{\pm} n_p^{\pm} e^{\frac{E^{\pm}-E_r^{\pm}}{k_B T}} - W_{\mathrm{XX}}(n_r^{\pm})^2(n_p^{\pm}+1) \pm W_{\mathrm{s}} \frac{e^{\frac{E_r^{\pm}-E_r^{\mp}}{k_B T}}}{1+e^{\frac{E_r^{\pm}-E_r^{\mp}}{k_B T}}}\left(n_r^{-} e^{\frac{E_r^{\pm}-E_r^{\mp}}{k_B T}} - n_r^{+}\right) - n_r^{\pm}/\tau_{\mathrm{r}} + P. \tag{4}$$

τ_{pol} and τ_{r} are the polariton and reservoir lifetime, W_{XX} the scattering rate from each spin reservoir into the ground state of the same spin component assisted mostly by exciton-exciton interactions and $D = \frac{S k_B T}{2\pi\hbar^2}$, S being the pillar surface. The scattering from the reservoir to the condensate is thus assumed to be spin conserving. The spin relaxation rate within the reservoir is given by W_{s}. We assume that the linearly polarized pump described by the term P introduces equal amounts of $\sigma^{\pm}$ excitons in the reservoir. One can notice that there is no spin relaxation term for the polariton state. While polariton condensates often demonstrate coherent spin precession induced by polarization splitting between linearly polarized eigenstates [9], this splitting is small in the pillar we consider and is neglected. The evolution of the system obtained within this model is shown as dotted lines for a magnetic field of $B = 9$ T in Figs. 3(c), 3(f), 3(j). Here the only fitting parameter is the spin relaxation rate W_{s}. Below condensation thresholds, most of the particles are in the

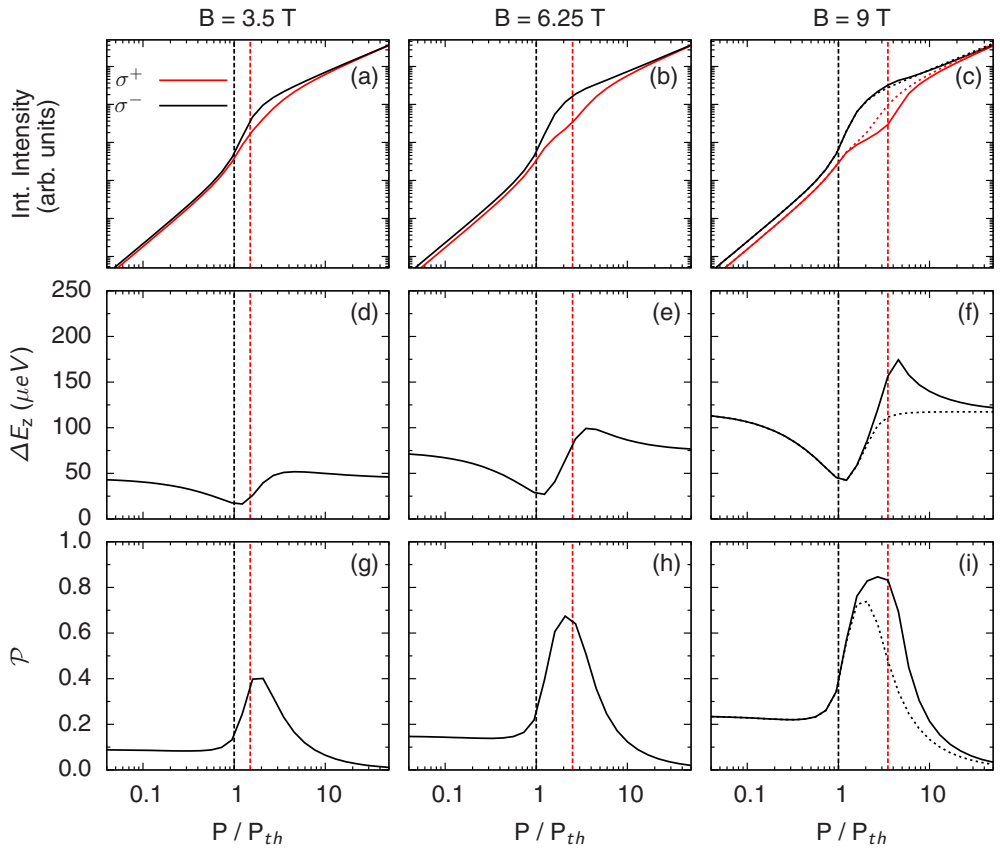

FIG. 3. (Color online) Simulations of the polariton emission intensity for both circular polarizations (a)–(c), Zeeman splitting (d)–(f) and degree of circular polarization (g)–(h) as a function of excitation power for three values of the magnetic field. The vertical dashed lines indicate condensation threshold for both circular polarizations. The dotted lines in (c), (f), (i) show numerical simulations taking into account constant scattering rates. The following parameters are used: $\tau_{\rm ph} = 10$ ps, $\tau_{\rm r} = 300$ ps, $\alpha_1 = 0.6\ \mu$eV, $\alpha_2 = -0.06\ \mu$eV, $W_{\rm XX} = 10^5\ {\rm s}^{-1}$, $W_{\rm s} = 4 \times 10^{10}\ {\rm s}^{-1}$, $\beta = 2.2 \times 10^{-3}\ {\rm cm}^2$, and $\delta = 2.2 \times 10^{-2}\ {\rm cm}^2$.

reservoir and the polariton population is very small. The total reservoir density grows as $P\tau_r$. Since the spin relaxation rate is faster than the scattering into the polariton states (i.e., $W_{\rm s} \gg W_{\rm XX} n_r$), the spin populations in the reservoir are close to equilibrium $n_r^+/n_r^- \approx \exp(\mu_B g B/k_B T)$. This finite polarization degree in the reservoir is responsible for the degree of circular polarization of 0.2 observed in the polariton emission. Such spin transfer from the reservoir to a polariton condensate, due to spin conservation in the energy relaxation of polaritons, is in line with the recent observations of circularly polarized condensates, without magnetic field, but under circular pumping [31]. Another consequence of the reservoir spin polarization is the renormalization of the polariton ZS. Indeed, below threshold, the ZS is approximately given by $x\mu_B g B_z + \alpha_1 x(n_r^+ - n_r^-)$. At very low density, the polariton ZS is thus equal to the exciton ZS weighted by the polariton exciton fraction. If n_r^+ exceeds n_r^-, the blue shift induced by the reservoir population is larger for σ^+ (the lowest-energy polariton state) than for σ^-. As a result, as the excitation density is increased, the ZS progressively decreases, as observed experimentally. In this regime, the polariton ZS can even change sign as recently reported [17] but with a different physical interpretation.

At some threshold density $n_r^{\rm th}$, the condensation occurs selectively in the more populated component σ^+. The scattering between the σ^+ reservoir and the σ^+ polariton states becomes stimulated, proportional to $W_{\rm XX} n_p^+$, and can thus easily exceed $W_{\rm s}$. Above $P_{\rm th}^+$, n_r^+ does not grow versus pumping, keeping its threshold value, because all extra particles introduced by the pumping are rapidly scattered to the condensate. $(n_p^+ + n_r^+)$ rises approximately as $P\tau_{\rm pol}$, $\tau_{\rm pol}$ being typically ten times smaller than the reservoir lifetime. The σ^+ condensation therefore leads to a strong reduction of the average time that a σ^+ particle spends in the system between absorption and emission. For $P_{\rm th}^+ < P < P_{\rm th}^-$, n_r^- continues to rise as $P\tau_r$, which is thus faster than the increase of the total density of spin-up particles given by $n_r^+ + n_p^+$. The reservoir population imbalance between the two spin components therefore reduces, which induces a rise of the ZS of the polariton mode. Both in the experiment and the theory, slightly above $P_{\rm th}^+$, the ZS reaches its minimum value and then increases. Interestingly, the condensate circular polarization degree continues to rise well beyond the ZS reaching its minimum. This demonstrates the absence of a simple connection between the circular polarization degree and the ZS, because of the complex role of the reservoir characterized by a finite spin relaxation time.

Increasing the pumping further leads to the condensation of the σ^- spin component. Within the simple set of equations presented above, the reservoir density required to trigger condensation is the same for both spin components. This means that reaching $P = P_{\text{th}}^-$, the total σ^- density is expected to remain smaller than the total σ^+ density. The ZS should therefore stay smaller than its low density value as shown by the calculation displayed in dotted lines. When increasing further the pumping, the relaxation rates accelerate and the two spin subsystems become more and more isolated. The same amount of σ^+ and σ^- being introduced by the pumping, they are scattered to the condensate and emitted by the condensate before any spin conversion can take place. The ZS therefore goes back to its low-density value and the circular polarization degree of the emission tends to zero. Each spin subsystem can be properly described by a thermodynamic equilibrium, which is not the case for the whole system because of the slow spontaneous spin relaxation rate. This last feature is clearly observed experimentally and reproduced by the above-described kinetic approach.

One experimental feature not reproduced by the model is the ZS pronounced maximum, which lies close to the σ^- threshold. If we assume that α_1 and α_2 are constant, the only possible explanation of the ZS maximum is that the σ^- total density in the system becomes larger than the σ^+ density. This means that the σ^- threshold is notably increased with respect to the σ^+ threshold. We also notice that the σ^- emission shows a plateau just after the σ^+ threshold, further indicating that the σ^- polariton relaxation is affected by the presence of the σ^+ condensate. This nonlinear change of the threshold is not expected from the set of equations (1)–(4). It implies a nonlinear decay of the lifetime and/or of the scattering rates versus the σ^+ condensate density. A nonlinear dependence of the scattering rates over densities can appear if higher-order terms are included in the derivation of Boltzmann equations or by taking into account spatial effects. Indeed the polariton scattering rates strongly depend on the overlap integrals between the polariton states and the reservoir. These overlaps can vary significantly in the condensation regime, as shown for instance in the case of focused excitation spots [8,27]. Several physical mechanisms, such as reservoir depletion or interaction-induced wave function change, may play a role simultaneously in the evolution of these overlap integrals. Their relative contributions are difficult to check experimentally with the setup used for the experiments presented here and beyond the scope of the present paper. As explained in Appendix B, these mechanisms lead in the first order to the same phenomenological nonlinear dependence of scattering rates on the polariton density, namely:

$$W_{\text{XX}}^{\mp} = W_{\text{XX}}^{0}\left(1 - \frac{\beta n_p^{\pm}}{1 + \delta n_p^{\mp}}\right), \tag{5}$$

The results of the simulations considering this non-linear mechanism and using β and δ as fitting parameters are shown with solid lines on Fig. 3. The plateau of the σ^- emission above the σ^+ threshold is reproduced together with the increase of the ZS above its low-density value. Thus, we infer that the pronounced maximum in the ZS is a signature of a nonlinear interplay between the two spin components. Further investigation would be necessary to verify the nature of this nonlinear coupling. Note that in the whole density regime explored here, polariton-exciton interactions are much stronger than polariton-polariton interactions. Therefore the ZS variations reflects modulations in the two reservoir densities.

V. CONCLUSION

To conclude, we have measured and described theoretically the polarization degree and ZS of a polariton condensate in a magnetic field in the Faraday configuration. This is of high importance, since the magnetic response of polaritons is a unique opportunity to manipulate photonic modes at optical frequencies using magnetic fields. We report a very strong impact of the spin anisotropic interactions on the condensation dynamics in the magnetic field. However, there is no pumping range in which the original spin-Meissner effect could be observed. This work shows that thermodynamic approaches, which give satisfactory descriptions in some limiting scalar cases, are not fully adapted to describe a spin polarized driven-dissipative condensate, essentially because of the long spin conversion rates. This can be seen as an opportunity to manipulate the spin of polariton condensates using either magnetic fields as in the present work or reservoirs pumped optically with circularly polarized light [31].

ACKNOWLEDGMENTS

We thank A. Kavokin for fruitful discussions. This work was partly supported by the FP7 ITN "Clermont4" (235114), by the ANR project Quandyde (ANR-11-BS10-001), by the French RENATECH network, by a public grant overseen by the French National Research Agency (ANR) as part of the "Investissements d'Avenir" program (Labex NanoSaclay, reference: ANR-10-LABX-0035), and the RTRA Triangle de la Physique contract "Boseflow1D" and "2012-039T-InterPol".

APPENDIX A: INTERACTION CONSTANTS

We describe below in more detail the assumptions used in the model concerning the different interaction constants.

We assume that the interactions between two exciton-polaritons with same spins are described by $x_1 x_2 \alpha_1$ where $x_{1,2}$ are the exciton fractions of the two interacting exciton-polaritons, and α_1 is the interaction constant for two excitons having the same spin. We assume exciton interactions in the reservoir to be spin-isotropic, so that the interaction constant between two reservoir excitons having opposite spins is also equal to α_1.

However, the interaction between exciton-polaritons with opposite spins is a second order process which passes through an intermediate state: either dark excitons or biexcitons. It approximately reads [9]: $\alpha_2 \approx |M|^2/\Delta E$, where ΔE is the difference between the energies of the interacting particles and of the intermediate state and M the matrix element of the exciton-exciton interaction. If we consider the interaction between two polaritons $\Delta E \sim -\Omega$, whereas for the interaction between a polariton and a reservoir exciton the energy difference is $\Delta E \sim \Omega/2$. The resulting interaction constant is

therefore about twice larger for exciton polariton interactions. We take $x^2\alpha_2$ the interaction constant between two polaritons, and $2x\alpha_2$ the interaction constant between a polariton and a reservoir exciton. However, one should notice that in our simulation the interaction between opposite spin particles always play negligible role because of the low value of α_2 and the low value of the condensate density with respect to the reservoir density in the explored range of excitation powers.

APPENDIX B: SPATIAL EFFECTS MODIFYING POLARITON RELAXATION

We propose here two nonlinear mechanisms, which could be responsible for the non-linear change of the scattering rates as described in the Eq. (5). In both cases, our goal is to obtain a correction of the scattering rates due to spatial effects, which is linear with n_p and saturates for large values of n_p.

Mechanism 1. This mechanism is induced by the drain of particles from the reservoir to the σ^+ condensate. The drain depletes the reservoir in a stronger way at the center of the pillar than on the edges. Since the resulting reservoir minimum is located exactly where the polariton wave function is maximal, it tends to reduce the effective scattering rate between the reservoir and the polariton state. Because of the spin conversion in the reservoir, the hole in the density also appears in the σ^- reservoir, inducing a decrease of the scattering rate, which in turn increases the σ^- condensation threshold. The σ^- reservoir therefore becomes more populated than the σ^+ one, which eventually leads to an increase of the Zeeman splitting above its low density value as observed experimentally.

Let us first describe this spatial effect within a single spin component, to simplify the picture. We can expect, that at large n_p, not all particles of the reservoir will be able to effectively scatter towards the condensate, because they will be mostly located in the areas where the condensate density is small (wave function tails). Let f be the fraction of the reservoir accessible in this limit:

$$W_{\mathrm{XX}} \underset{n_p\to\infty}{\longrightarrow} f W_{\mathrm{XX}}\,. \tag{B1}$$

Then, in order to provide this saturation and to remain linear in n_p, the correction has to be written as:

$$W_{\mathrm{XX}} = W^0_{\mathrm{XX}}\left(1-(1-f)\frac{n_p}{c+n_p}\right) \tag{B2}$$

where c is a constant, whose dimensionality is that of the number of particles which should be proportional to the reservoir density at threshold $c=\xi n_{r0}$ and describes the efficiency of the mechanism at low n_p. Eq. (B2) can be reformulated as

$$W_{\mathrm{XX}} = W^0_{\mathrm{XX}}\left(1-\frac{\beta n_p}{1+\delta n_p}\right), \tag{B3}$$

where $\beta=(1-f)/\xi n_{r0}$, $\delta=1/\xi n_{r0}$ can be used as two fitting parameters. Mechanism 1 can take place within a single spin component as written above. However, because of the spin conversion in the reservoir, the depletion of one spin component also induces depletion for the other spin component in the reservoir. Thus Eq. (B3) can be reformulated as follows for the scattering within a single spin component (condensate and reservoir of same spin):

$$W^{\pm,\pm}_{\mathrm{XX}} = W^0_{\mathrm{XX}}\left(1-\frac{\beta n_p^{\pm}}{1+\delta n_p^{\pm}}\right), \tag{B4}$$

where the first (second) index for W_{XX} refers to the spin of the polariton state (reservoir). On the other hand, the inter-spin scattering is formulated as follows:

$$W^{\pm,\mp}_{\mathrm{XX}} = W^0_{\mathrm{XX}}\left(1-\frac{\beta n_p^{\mp}}{1+\delta n_p^{\pm}}\right). \tag{B5}$$

This last formula describing interspin scattering, is nothing else but the Eq. (5) where for simplicity we have omitted the index of the reservoir spin. In fact, the correction induced on the inter-spin scattering is the only one which is relevant for the present study. It is more important both in its values and its consequences, than the correction within a single spin component. Indeed, a small decrease of the scattering rate of the component above its threshold is masked by a nonlinear increase of the relaxation due to the stimulation. On the other hand, when the component is not yet condensed, its dynamics is much more sensitive to a decrease of its scattering rate.

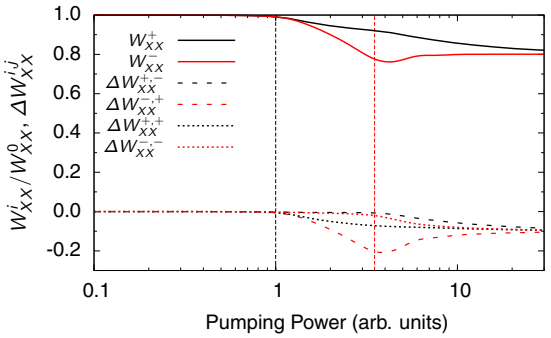

FIG. 4. (Color online) (Solid lines) Total normalized scattering rate into the + and − polariton states as a function of excitation power including mechanism 1; (dotted and dashed lines) Correction to the scattering rate, $\Delta W^{i,j}_{\mathrm{XX}} = \frac{W^{i,j}_{\mathrm{XX}} - W^0_{\mathrm{XX}}}{W^0_{\mathrm{XX}}}$, for the two interspin and intraspin components including mechanism 1. i (j) refers to the spin of the polariton state (reservoir). The vertical black (red) dashed line indicates condensation threshold for σ^+ (σ^-) polarization $B = 9$T.

This is illustrated in Fig. 4 where we show the relative importance of the various contributions, calculated with the same parameters β and δ as for the simulation of the experimental data, i.e. $\beta = 2.2\times10^{-3}\,\mathrm{cm}^2$, $\delta = 2.2\times10^{-2}\,\mathrm{cm}^2$. Clearly the most important effect of mechanism 1 is due to the action of the majority component on the minority one (red dashed line). Since the variation of the scattering rates occurs for excitation powers above the σ^+ condensation threshold, it increases the threshold value for σ^- polaritons and, consequently, the measured Zeeman splitting.

Mechanism 2. This mechanism is based on the spin-anisotropic polariton-polariton interactions. The central

hypothesis is that a σ^+ condensate with approximately a cosine wave function forms at the center of the pillar. This condensate interacts attractively with the σ^- polaritons through the α_2 constant. The σ^- polariton wave function is therefore expected to be more localized in real space than in the absence of the σ^+ condensate, which reduces its overlap integral with the reservoir which is almost homogeneous, with a small depletion at the center of the pillar as mentioned above. Again this decreasing of the overlap integral reduces the scattering rate involving the σ^- particles, once the σ^+ condensate becomes strongly occupied.

In this case, we can assume that the scattering rate is reduced proportionally to the relative width of the condensate wave function with respect to the size of the reservoir (size of the pillar). The relative shrinking of the σ^- wave function due to the interactions with σ^+ is calculated by using the perturbation theory. At low n_p^+, it is proportional to $\alpha_2 n_p^+/E_c$, where E_c is the localization energy of the condensate $E_c = \pi^2\hbar^2/mL^2$, where L and m are the pillar size and mass of the polaritons, respectively. As the interactions in σ^- become important, the efficiency of the scattering rate is described by the competition between the repulsion $\alpha_1 n_p^-$ within σ^- (because the repulsive interactions due to α_1 lead to the spreading of the wave function towards the Thomas-Fermi profile) and contraction due to σ^+. The effect of this competition on the σ^- population scattering rate can be expressed as follows:

$$W_{XX}^- = W_{XX}^0\left(1+\frac{\alpha_2 n_p^+}{E_c+\alpha_1 n_p^-}\right) = W_{XX}^0\left(1-\frac{\beta n_p^+}{1+\delta n_p^-}\right). \tag{B6}$$

Here we only wrote the interspin component since we have seen that this is the one that strongly affects the scattering rates for powers between the two thresholds. Notice that in mechanism 1 and 2, we assume a polariton wave function with a maximum at the pillar center. In Ref. [8], we reported that when the excitation spot is much smaller than the pillar size, repulsive interaction with the excitonic reservoir tends to push the condensate away from the pillar center and a pronounced dip develops at the center of the condensate wave function. Nevertheless this effect does not occur when the excitation spot is of the same order than the diameter. This is shown in the supplementary material of Ref. [8] for a 3.2 μm diameter. So, for the pillar and excitation spot dimensions considered in the present work, we can safely assume a polariton wave function peaked at the center for the entire range of excitation powers.

[1] A. J. van Doorn, M. van Exter, M. Travagnin, and J. Woerdman, Polarization behavior of surface-emitting semiconductor lasers in an axial magnetic field, Opt. Commun. **133**, 252 (1997).

[2] F. D. M. Haldane and S. Raghu, Possible realization of directional optical waveguides in photonic crystals with broken time-reversal symmetry, Phys. Rev. Lett. **100**, 013904 (2008).

[3] A. Khanikaev, S. Mousavi, W.-K. Tse, M. Kargarian, A. MacDonald, and G. Shvets, Photonic topological insulators, Nature Mater. **12**, 233 (2013).

[4] A. Armitage, T. A. Fisher, M. S. Skolnick, D. M. Whittaker, P. Kinsler, and J. S. Roberts, Exciton polaritons in semiconductor quantum microcavities in a high magnetic field, Phys. Rev. B **55**, 16395 (1997).

[5] J. Tignon, P. Voisin, C. Delalande, M. Voos, R. Houdré, U. Oesterle, and R. P. Stanley, From Fermi's Golden rule to the Vacuum Rabi splitting: Magnetopolaritons in a semiconductor optical microcavity, Phys. Rev. Lett. **74**, 3967 (1995).

[6] D. D. Solnyshkov, M. M. Glazov, I. A. Shelykh, A. V. Kavokin, E. L. Ivchenko, and G. Malpuech, Magnetic field effect on polarization and dispersion of exciton-polaritons in planar microcavities, Phys. Rev. B **78**, 165323 (2008).

[7] A. Rahimi-Iman, C. Schneider, J. Fischer, S. Holzinger, M. Amthor, S. Höfling, S. Reitzenstein, L. Worschech, M. Kamp, and A. Forchel, Zeeman splitting and diamagnetic shift of spatially confined quantum-well exciton polaritons in an external magnetic field, Phys. Rev. B **84**, 165325 (2011).

[8] L. Ferrier, E. Wertz, R. Johne, D. D. Solnyshkov, P. Senellart, I. Sagnes, A. Lemaître, G. Malpuech, and J. Bloch, Interactions in confined polariton condensates, Phys. Rev. Lett. **106**, 126401 (2011).

[9] I. A. Shelykh, A. V. Kavokin, Y. G. Rubo, T. C. H. Liew, and G. Malpuech, Polariton polarization-sensitive phenomena in planar semiconductor microcavities, Semicond. Sci. Technol. **25**, 013001 (2010).

[10] N. Takemura, S. Trebaol, M. Wouters, M. Portella-Oberli, and B. Deveaud, Polaritonic Feshbach resonance, Nat. Phys. **10**, 500 (2014).

[11] I. A. Shelykh, Y. G. Rubo, G. Malpuech, D. D. Solnyshkov, and A. Kavokin, Polarization and propagation of polariton condensates, Phys. Rev. Lett. **97**, 066402 (2006).

[12] J. Kasprzak, M. Richard, S. Kundermann, A. Baas, P. Jeambrun, J. M. J. Keeling, F. M. Marchetti, M. H. Szymanska, R. Andre, J. L. Staehli, V. Savona, P. B. Littlewood, B. Deveaud, and L. S. Dang, Bose–Einstein condensation of exciton polaritons, Nature (London) **443**, 409 (2006).

[13] J. Kasprzak, R. André, L. S. Dang, I. A. Shelykh, A. V. Kavokin, Y. G. Rubo, K. V. Kavokin, and G. Malpuech, Build up and pinning of linear polarization in the Bose condensates of exciton polaritons, Phys. Rev. B **75**, 045326 (2007).

[14] Y. G. Rubo, Suppression of superfluidity of exciton-polaritons by magnetic field, A. Kavokin, and I. Shelykh, Phys. Lett. A **358**, 227 (2006).

[15] P. Walker, T. C. H. Liew, D. Sarkar, M. Durska, A. P. D. Love, M. S. Skolnick, J. S. Roberts, I. A. Shelykh, A. V. Kavokin, and D. N. Krizhanovskii, Suppression of Zeeman splitting of the energy levels of exciton-polariton condensates in semiconductor microcavities in an external magnetic field, Phys. Rev. Lett. **106**, 257401 (2011).

[16] A. V. Larionov, V. D. Kulakovskii, S. Höfling, C. Schneider, L. Worschech, and A. Forchel, Polarized nonequilibrium Bose-Einstein condensates of spinor exciton polaritons in a magnetic field, Phys. Rev. Lett. **105**, 256401 (2010).

[17] J. Fischer, S. Brodbeck, A. V. Chernenko, I. Lederer, A. Rahimi-Iman, M. Amthor, V. D. Kulakovskii, L. Worschech, M. Kamp, M. Durnev, C. Schneider, A. V. Kavokin, and S. Höfling, Anomalies of a nonequilibrium spinor polariton condensate in a magnetic field, Phys. Rev. Lett. **112**, 093902 (2014).

[18] J. Kasprzak, D. D. Solnyshkov, R. André, L. S. Dang, and G. Malpuech, Formation of an exciton polariton condensate: Thermodynamic versus kinetic regimes, Phys. Rev. Lett. **101**, 146404 (2008).

[19] Feng Li, L. Orosz, O. Kamoun, S. Bouchoule, C. Brimont, P. Disseix, T. Guillet, X. Lafosse, M. Leroux, J. Leymarie, M. Mexis, M. Mihailovic, G. Patriarche, F. Réveret, D. Solnyshkov, J. Zuniga-Perez, and G. Malpuech, From excitonic to photonic polariton condensate in a ZnO-based microcavity, Phys. Rev. Lett. **110**, 196406 (2013).

[20] M. Assmann, J.-S. Tempel, F. Veit, M. Bayer, A. Rahimi-Iman, A. Loffler, S. Hofling, S. Reitzenstein, L. Worschech, and A. Forchel, From polariton condensates to highly photonic quantum degenerate states of bosonic matter, PNAS **108**, 1804 (2011).

[21] K. Kamide and T. Ogawa, Ground-state properties of microcavity polariton condensates at arbitrary excitation density, Phys. Rev. B **83**, 165319 (2011).

[22] M. H. Szymańska, J. Keeling, and P. B. Littlewood, Nonequilibrium quantum condensation in an incoherently pumped dissipative system, Phys. Rev. Lett. **96**, 230602 (2006).

[23] D. Solnyshkov, I. Shelykh, M. Glazov, G. Malpuech, T. Amand, P. Renucci, X. Marie, and A. Kavokin, Nonlinear effects in spin relaxation of cavity polaritons, Semiconductors **41**, 1080 (2007).

[24] D. V. Vishnevsky, D. D. Solnyshkov, N. A. Gippius, and G. Malpuech, Multistability of cavity exciton polaritons affected by the thermally generated exciton reservoir, Phys. Rev. B **85**, 155328 (2012).

[25] D. Bajoni, P. Senellart, E. Wertz, I. Sagnes, A. Miard, A. Lemaître, and J. Bloch, Polariton laser using single micropillar GaAs−GaAlAs semiconductor cavities, Phys. Rev. Lett. **100**, 047401 (2008).

[26] A. V. Kavokin, J. J. Baumberg, G. Malpuech, and F. P. Laussy, *Microcavities*, edited by R. J. Nicholas and H. Kamimura (Oxford University Press, Oxford, 2007).

[27] M. Galbiati, L. Ferrier, D. D. Solnyshkov, D. Tanese, E. Wertz, A. Amo, M. Abbarchi, P. Senellart, I. Sagnes, A. Lemaître, E. Galopin, G. Malpuech, and J. Bloch, Polariton condensation in photonic molecules, Phys. Rev. Lett. **108**, 126403 (2012).

[28] M. I. D'yakonov and V. I. Perel', Fiz. Tverd. Tela **13**, 3581 (1971) [Spin relaxation of conduction electrons in noncentrosymmetric semiconductors, Sov. Phys. Solid State **13**, 3023 (1972)].

[29] M. Z. Maialle, E. A. de Andrada e Silva, and L. J. Sham, Exciton spin dynamics in quantum wells, Phys. Rev. B **47**, 15776 (1993).

[30] M. Vladimirova, S. Cronenberger, D. Scalbert, K. V. Kavokin, A. Miard, A. Lemaitre, J. Bloch, D. Solnyshkov, G. Malpuech, and A. V. Kavokin, Polariton-polariton interaction constants in microcavities, Phys. Rev. B **82**, 075301 (2010).

[31] E. Kammann, T. C. H. Liew, H. Ohadi, P. Cilibrizzi, P. Tsotsis, Z. Hatzopoulos, P. G. Savvidis, A. V. Kavokin, and P. G. Lagoudakis, Nonlinear optical spin hall effect and long-range spin transport in polariton lasers, Phys. Rev. Lett. **109**, 036404 (2012).